Lasers in Surgery and Medicine 40:716–725 (2008)

Solder Doped Polycaprolactone Scaffold Enables Reproducible Laser Tissue Soldering

Amadé Bregy, MD,[1] Serge Bogni, MSc,[2] Vianney J.P. Bernau, MSc,[3] Istvan Vajtai, MD,[4] Felix Vollbach, MS,[5] Alke Petri-Fink, PhD,[3] Mihai Constantinescu, MD,[5] Heinrich Hofmann, Dr.Ing.,[3] Martin Frenz, PhD,[2]* and Michael Reinert, MD[1]

[1]*Department of Neurosurgery, Inselspital Bern, University of Bern, 3010 Bern, Switzerland*
[2]*Institute of Applied Physics, University of Bern, 3012 Bern, Switzerland*
[3]*Laboratory of Powder Technology, École Polytechnique Fédérale de Lausanne, 1015 Lausanne, Switzerland*
[4]*Department of Pathology, Inselspital Bern, University of Bern, 3010 Bern, Switzerland*
[5]*Department of Plastic and Reconstructive Surgery, Inselspital Bern, University of Bern, 3010 Bern, Switzerland*

Background and Objectives: In this in vitro feasibility study we analyzed tissue fusion using bovine serum albumin (BSA) and Indocyanine green (ICG) doped polycaprolactone (PCL) scaffolds in combination with a diode laser as energy source while focusing on the influence of irradiation power and albumin concentration on the resulting tensile strength and induced tissue damage.

Materials and Methods: A porous PCL scaffold doped with either 25% or 40% (w/w) of BSA in combination with 0.1% (w/w) ICG was used to fuse rabbit aortas. Soldering energy was delivered through the vessel from the endoluminal side using a continuous wave diode laser at 808 nm via a 400 μm core fiber. Scaffold surface temperatures were analyzed with an infrared camera. Optimum parameters such as irradiation time, radiation power and temperature were determined in view of maximum tensile strength but simultaneously minimum thermally induced tissue damage. Differential scanning calorimetry (DSC) was performed to measure the influence of PCL on the denaturation temperature of BSA.

Results: Optimum parameter settings were found to be 60 seconds irradiation time and 1.5 W irradiation power resulting in tensile strengths of around 2,000 mN. Corresponding scaffold surface temperature was $117.4 \pm 12^{\circ}$C. Comparison of the two BSA concentration revealed that 40% BSA scaffold resulted in significant higher tensile strength compared to the 25%. At optimum parameter settings, thermal damage was restricted to the adventitia and its interface with the outermost layer of the tunica media. The DSC showed two endothermic peaks in BSA containing samples, both strongly depending on the water content and the presence of PCL and/or ICG.

Conclusions: Diode laser soldering of vascular tissue using BSA-ICG-PCL-scaffolds leads to strong and reproducible tissue bonds, with vessel damage limited to the adventitia. Higher BSA content results in higher tensile strengths. The DSC-measurements showed that BSA denaturation temperature is lowered by addition of water and/or ICG-PCL. Lasers Surg. Med. 40:716–725, 2008. © 2008 Wiley-Liss, Inc.

Key words: albumin; biodegradable polymer; diode laser; indocyanine green; tensile strength

INTRODUCTION

During the last 40 years a focus in research was put on sutureless tissue fusion, to handle the limits of conventional suturing such as vascular wall damage due to the penetrating needle, intraluminal foreign body reactions caused by non-absorbable suture material and thrombocyte aggregation, impaired endothelial function, intimal hyperplasia and hence stenosis [1–6]. Sutured wounds have greater and longer duration inflammatory response than laser soldered wounds [7,8]. Furthermore suturing does not create a watertight connection, which can, for example, in visceral surgery lead to an entry for pathogens resulting in severe complications such as infections or death [9].

The trend in modern surgery towards endoscopic and minimally invasive approaches requires adaptation of the surgical instruments and techniques. The method of tissue adaptation is therefore limited by free moving space thus revealing conventional suturing unsuitable. Fibrin based adhesives or glues achieve insufficient tensile strength for suture replacement and are further limited by early resorption [10,11]. These products can be used as temporary sealants or hemostatic agents. Cyanoacrylate based adhesives offer sufficient tensile strength, but are limited by toxicity [12], allergic reaction, anaphylaxis [13,14] and immediate polymerization properties, precluding a precise surgical application. An excellent review on different laser soldering and welding techniques has been published by McNally [15].

Contract grant sponsor: Swiss National Foundation; Contract grant number: 3200B0-107611.
*Correspondence to: Prof. Dr. Martin Frenz, PhD, Institute of Applied Physics, Sidlerstrasse 5, 3012 Bern, Switzerland.
E-mail: martin.frenz@iap.unibe.ch
Accepted 13 August 2008
Published online in Wiley InterScience (www.interscience.wiley.com).
DOI 10.1002/lsm.20710

Laser assisted vascular anastomosis was already introduced in 1964 by Yahr et al. [16], yet a broad clinical use has still not been achieved [17–25]. The introduction of a chromophore enhanced protein solder [26,27] for selective energy absorption and temperature activated adhesion properties, increased tensile strength and reduced tissue damage due to lower soldering temperature. However, fusion of solder and tissue needs minimal temperatures allowing achievement of molecular mobility, which permits intermingling of the protein helices and polymerization [28]. Biodegradable polymers such as polyglycolic acid [7,29–31] or addition of natural and synthetic crosslinkers such as genipin [32] have been studied and resulted in increased tensile strength. However, most of these combinations harbored a liquid solder, which run off during soldering. This caused inhomogenous and insufficient energy absorption and thus poor reproducibility and thermal damage of surrounding tissue. To prevent the runaway of the solder and to increase the absorbed energy density at the point of interest, we introduced a dry polycaprolactone (PCL) scaffold doped with bovine serum albumin (BSA) and Indocyanine Green (ICG) (BIP-scaffold). The hypothesis was to obtain a more localized energy deposition and protein immobilization thus leading to stronger and more reproducible tensile strengths. The goal was to determine optimum parameter settings leading to a maximum in tensile strength and minimum in tissue damage in order to further improve our intraluminal laser soldering technique [33].

MATERIALS AND METHODS

Scaffold Production

Porous PCL (M_n 80,000 (GPC), Sigma–Aldrich Chemie GmBH, Steinheim, Germany) membranes were produced using the solvent casting and particulate leaching technique [34]. After complete dissolving of 501.45 mg of PCL in 15 ml of chloroform (Purity 99.0–99.4%, MERCK, Darmstadt, Germany) using a magnetic stirrer, 5.546 g of sodium chloride (reinst, Ph Eur III, Dr. Grogg Chemie AG, Stettlen, Switzerland) sieved to a particle size of 100–150 μm were added to produce membranes of desired porosity [34]. The resulting suspension was cast into a petri dish of 95 mm diameter and then left under the fume hood for 24 hours to evaporate the chloroform. Afterwards it was washed for 24 hours in ultra pure water. The polymer scaffold was then carefully peeled off the bottom of the petri dish and immersed again in ultra pure water, which was changed 3–4 times during 24 hours to leach out all the remaining salt particles. The resulting membrane was air dried before incubating in 20 ml of solder in a sealed round container, which was kept moving for 24 hours on a slow rotator for homogenous solder-soaking. The resulting scaffolds were extracted and put onto a Teflon foil. The solder surplus was carefully removed using a spatula since otherwise it would lead to inhomogenities and brittleness of the scaffold. Then the scaffolds were again air-dried and stored light proven until use. For the experiments, a custom made cutting device was used to cut the dry, solder doped polymer scaffolds with a razor blade to a dimension of 5 mm × 10 mm. The device allowed a precise cutting of the pieces with minimal damage to the scaffold structure.

Solder Preparation

Twenty-five and 40% (w/w) BSA (Sigma–Aldrich) respectively were dissolved in ultra pure water, together with 0.1% (w/w) of ICG (Acros Organics-Janssen Pharmaceuticals, Geel, Belgium) using a magnetic stirrer and a water bath of 37°C for 12 hours. Because of its high viscosity, the 40% solution was prepared in two steps. Half of the amount of protein was dissolved in the ultra pure water for 2 hours, subsequently the second half was added. The resulting solder was stored light proven and cooled at 4°C until use. Solder not used within 1 week was discarded [26].

Laser Source and Light Delivery System

As laser source a GaAlAs (gallium aluminum arsenide) diode laser system (DL50, FISBA Optik, St. Gallen, Switzerland) emitting continuous wave radiation in the near infrared at $\lambda = 808$ nm was used. The light was coupled into a 400 μm multimode quartz fiber (NA = 0.2). The vessels were soldered from the intimal side through the vessel wall at a distance of 13 mm to the fiber, resulting in an irradiation spot diameter of 5.2 mm. The power output was measured using a power meter (Power Max PM500D, Molectron, Portland, OR). Laser power used was in the range of 0.6–3 W corresponding to an irradiance between 2.8 and 14.1 W/cm^2. The irradiation time was between 10 and 240 seconds.

Temperature Measurements

For temperature recording an infrared camera (Radiance HS, Raytheon, Waltham, MA) calibrated for a temperature range between 0°C and 145°C allowing an accuracy of ± 1% was used. The camera controlling and data recording was performed using Image Desk II software. Analysis and data processing was performed using IDL 6.2. Temperatures were recorded at the surface of the BIP-scaffold (Fig. 1).

Tissue Preparation

All experiments were performed using rabbit aortic arteries (Zika-hybrid rabbits, 11–13 weeks old), which were freshly obtained from a local slaughterhouse. The rabbit aortic arteries were kept in a 0.1 M phosphate buffered saline (PBS, pH 7.4) imbued gauze at 4°C until further use. All the experiments were performed within the first 24 hours after extraction of the arteries. Prior to use, the surrounding fatty tissue and the loose adventitial surrounding the arteries was carefully removed using microsurgical instruments. Tensile strengths of native vessels were assessed using fresh lengthwise cut vessels, opened and shortened to a dimension of 8 mm × 20 mm ($n = 15$). For comparison, all experiments were additionally done with previously frozen vessels. For that reason the aortic arteries were frozen in the same protein buffered solution imbued gauze at −80°C. Before using the arteries, they were defrosted slowly to room temperature.

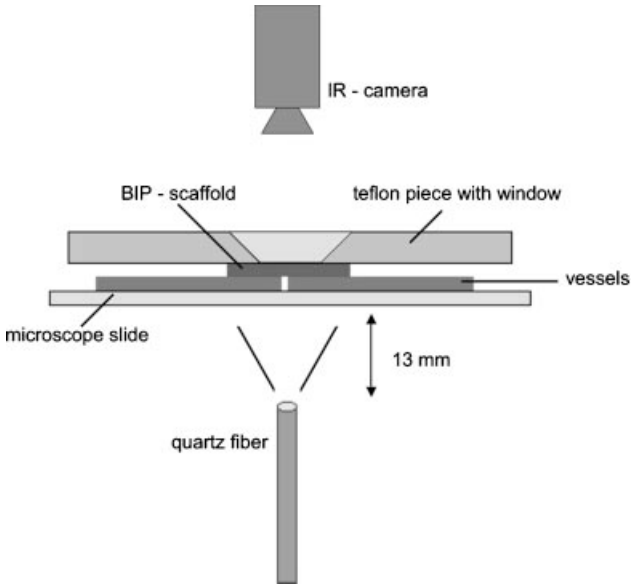

Fig. 1. Scheme of the soldering setup. Two pieces of aortic vessels were mounted with the adventitial side upwards onto a microscope slide with the BIP-scaffold placed on top. To keep the scaffold-tissue system plane, a thin Teflon plate with a hole for surface temperature recording was placed on top. Soldering was performed from the bottom through the aortic tissue using near infrared diode laser ($\lambda = 808$ nm) radiation transmitted through a 400 μm core fiber. The spot on the tissue bottom had a diameter of 5.2 mm. During soldering process, the scaffold surface temperature was recorded using an infrared camera.

Soldering Procedure

For the soldering procedure, the aortic arteries were cut lengthwise, opened and shortened to pieces of 8 mm×10 mm. After placing the two artery pieces end-to-end on a microscope slide, the polymer scaffold was put on top of the adventitia of the two vessel pieces. On top of this tissue-scaffold sandwich, a thin Teflon plate (weight 20 g) with a hole (diameter = 8 mm) for temperature observation was placed, in order to guarantee close and standardized contact between the polymer scaffold and the tissue (Fig. 1). Laser irradiation was performed from the endoluminal side. Three to six specimens were tested for each combination of incident laser power and irradiation time. The four groups of different polymer scaffolds and fresh as well as previously frozen tissue had a sample size of 15 specimens per group. The tensile strength was measured within 1 minute after soldering to avoid changes in repair strength associated with drying [35].

Tensile Strength Assessment

A test stand with a fixed force gauge (BFG50, Mecmesin Limited, West Sussex, United Kingdom) was used to measure tensile strengths. The tissue was fixed by two surgical clamps attached to a moving table, which was pulled using an electrically driven motor at a constant velocity of 27 mm/minute.

Differential Scanning Calorimetry (DSC)

The experiments were performed using a Mettler DSC 25 calorimeter connected to a Mettler Toledo TC15 TA controller (Mettler-Toledo, Greifensee, Switzerland). Standard aluminum 40 μl crucibles were used. All DSC scans were run from 45 to 200°C at a heating rate of 10°C/minute and an air flow of 100 ml/minute. Measured samples were native BSA, native porous PCL scaffold and the BIP-scaffold, used in the experiments. The samples were stored in a climatic test cabinet (Rumed GmbH, Laatzen, Germany) at different humidity levels. Moisture contents were measured gravimetrically until constant weight.

Scanning Electron Microscopy

Scanning electron microscopy was performed from the top surface (exposed to air in the petri dish) of PCL scaffolds. Therefore the scaffold samples were prepared by affixing them on specimen mounts with conduction carbon tabs (Plano, Wetzlar, Germany) and coated with gold in an argon atmosphere at 220 V and 40 mA for 1 minute in a sputter coater (coating thickness of approximately 20 nm) (Bal-Tec AG, Balzers, Liechtenstein). Electron microscopy was performed on an ISI-DS 130S scanning electron microscope at 20 kV (Lights, Wetzlar, Germany). Micrographs were recorded with a digital image processing system (DISP, point electronic GmbH, Halle, Germany).

Histology

Assessment of histological aspects of laser-induced thermal damage to vessel wall was performed using light microscopy in a diagnostic surgical pathology setting. Immediately after soldering, tissue samples were fixed overnight in 5% buffered aqueous solution of formaldehyde, and routinely processed to paraffin. Consecutive serial sections of 3 μm thickness were alternately stained with hematoxylin–eosin (H&E) and van Gieson's elastic method (EvG). Standard treated vessels were irradiated with 1.5 W during 60 seconds, whereas overheated samples were irradiated with 1.5 W but during 240 seconds.

Statistical Analysis

The data were analyzed by two-tailed Student's t-test for unpaired observations and the two-way ANOVA test with Bonferroni posttest, using GraphPad Prism 5 software (San Diego). Differences with $P<0.05$ were considered as to be statistically significant. Values are reported as (mean ± SD), unless otherwise specified.

RESULTS

Polymer Scaffold

To measure the effective BSA-ICG content in the PCL scaffolds, the native porous scaffolds as well as the dried BIP-scaffolds were balanced. The weight of a cut BIP-scaffold was 19.42 ± 1.96 mg ($n = 10$) for a 40% BSA scaffold

and 8.19 ± 0.28 mg ($n = 10$) for a 25% BSA scaffold whereas a native PCL scaffold of same dimensions weighted 3.33 ± 0.17 mg ($n = 10$). The effective amount of BSA in the scaffold was therefore approximately 16 mg in the 40% BSA scaffold and 5 mg in the 25% BSA scaffold.

Scanning electron microscopy of the surface of polymer scaffolds (Fig. 2) showed open or partially filled pores in the native PCL scaffold and in the dried 25% BSA scaffold, respectively. In contrast, almost all the pores were entirely filled when doped with 40% BSA/ICG solution.

The tensile strength of 60 seconds denaturated BIP-scaffolds was $6{,}329 \pm 577$ mN whereas the tensile strength of the non-irradiated BIP-scaffolds was $5{,}098 \pm 221$ mN ($n = 6$), which is still stronger than the mean tensile strength of 15 native, non-irradiated aortas of 2 cm length which resulted in $3{,}805 \pm 1{,}145$ mN.

Tensile Strength Depending on Irradiation Time and Power

The tensile strength was found to depend on the energy deposition, which means a longer irradiation time or a higher intensity resulted in increased tensile strength. A maximum was found, after which further irradiation did not lead to higher tensile strengths (Fig. 3).

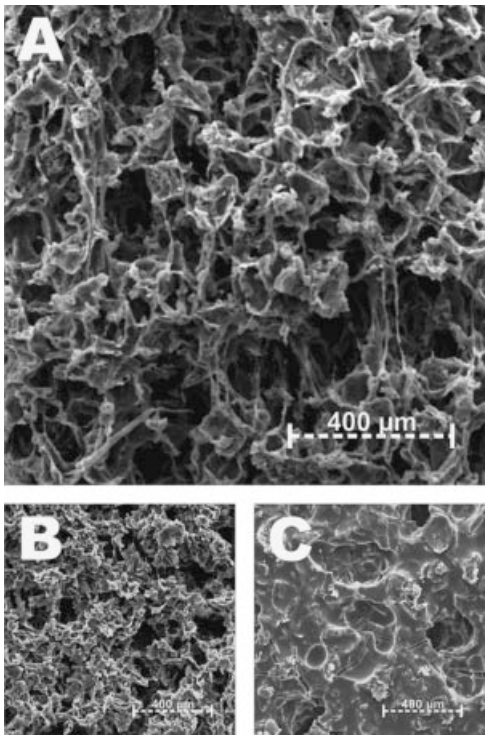

Fig. 2. Scanning electron microscopy of porous PCL polymer scaffolds. **A**: Surface of a native scaffold showing pore morphology. **B**: Detail of the surface of a polymer scaffold soaked with the 25% (w/w) BSA/ICG solder. **C**: Detail of the surface of a polymer scaffold soaked with the 40% (w/w) BSA/ICG solder.

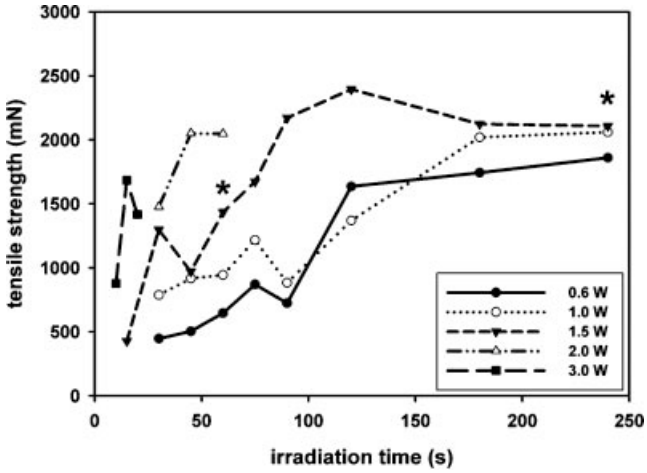

Fig. 3. Tensile strengths of soldered tissue vessels as a function of soldering time for different laser powers. A higher energy deposition (either due to longer irradiation time or higher intensity) leads to a higher tensile strength. The two asterisks mark the irradiation parameters and resulting tensile strength of the soldered samples used for histology (Fig. 7).

Tensile Strength Depending on Solder- and Vessel Type

Tensile strengths of the soldered tissue using the 40% BSA scaffold were significantly higher (fresh: $1{,}958 \pm 415$ mN, frozen: $2{,}091 \pm 470$ mN) compared to the 25% BSA scaffold (fresh: $1{,}580 \pm 302$ mN, frozen: $1{,}483 \pm 350$ mN) with $P = 0.0080$ for fresh and $P = 0.0004$ for the previously frozen tissue. These measurements were performed using a laser power of 1.5 W and an irradiation time of 60 seconds (Fig. 4). In almost all cases the rupture took place at the interface between the vessel wall and the scaffold.

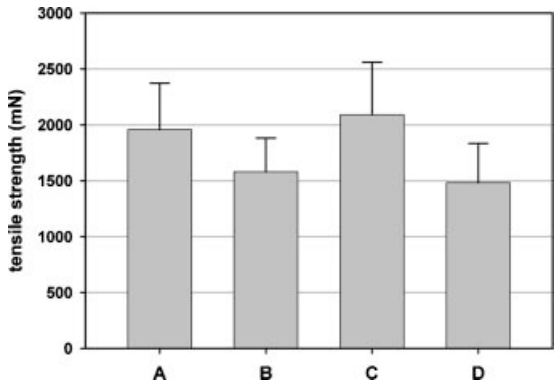

Fig. 4. The plot shows the tensile strength of fresh (**A**,**B**) and previously frozen tissue samples (**C**,**D**) soldered using the 40% and 25% BIP-scaffold. (A) represents 40% BSA scaffold and fresh tissue ($1{,}958 \pm 415$ mN), (B) represents 25% BSA scaffold and fresh tissue ($1{,}580 \pm 302$ mN), (C) represents 40% BSA scaffold and previously frozen tissue ($2{,}091 \pm 470$ mN) and (D) represents 25% BSA scaffold and previously frozen tissue ($1{,}483 \pm 350$ mN).

A comparison between fresh and previously frozen tissue samples for soldering showed no significant difference in tensile strength: $P = 0.4169$ for the 40% BSA scaffold and $P = 0.4246$ for the 25% BSA scaffold, respectively.

The F-test revealed that the variances in all four groups were not statistically significant different from each other ($0.25 < P < 0.65$).

Hydration of soldered aorta samples for 24 hours at room temperature in liquid 0.1 M phosphate buffered saline resulted in a decrease of tensile strength of around 50%.

Tests using only an ICG doped scaffold without BSA totally failed. Although the PCL membrane melts at 60°C we were not able to obtain any fusion independent of the laser parameters used, which clearly reveals that the BSA is mainly responsible for the soldering process.

Temperatures

The observed polymer surface temperature during soldering using the different irradiation parameters was in a range between 57°C and out of the calibrated detection range of the infrared camera which means higher than 145°C. The higher the laser power or the longer the irradiation time the higher was the maximum surface temperature on the polymer scaffold and the shorter the time to reach it (Fig. 5). The tensile strengths of all measured samples using different laser powers and different irradiation times were significantly correlated with soldering temperatures with a Pearson's correlation coefficient of $r = 0.7450$ ($P < 0.0001$) and with a linear regression curve of $y = 18.572x - 610.94$ ($r^2 = 0.5550$, $P < 0.0001$). The soldering of the 25% or the 40% BSA scaffolds at a laser power of 1.5 W and an irradiation time of 60 seconds resulted in a polymer surface temperature of 117.4 ± 12°C without statistically significant difference for both types of doped scaffolds ($P = 0.0686$, all $P > 0.05$ respectively).

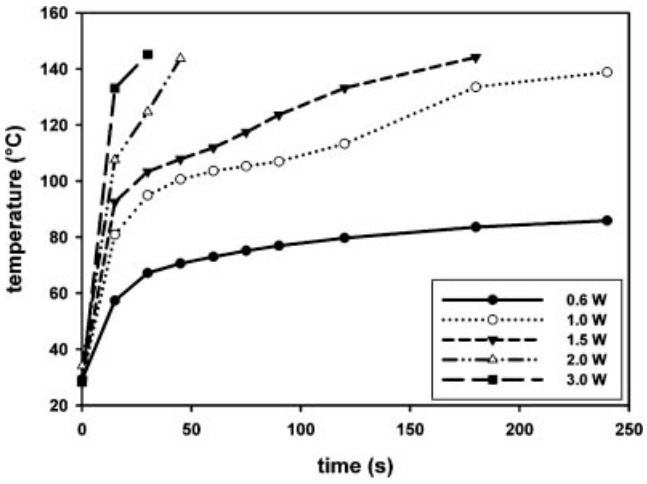

Fig. 5. Recorded maximum surface temperature as a function of irradiation time for different laser power. Calibrated detection range of the infrared camera was 0–145°C with an accuracy of ±1%.

Differential Scanning Calorimetry (DSC)

Figure 6a,b shows the DSC scans for the three different samples (BSA, PCL, BSA-ICG-PCL) equilibrated at 25°C at different moisture contents. The typical PCL melting point (T_m) is found at 60°C for the three polymer containing samples and is independent of the water content or the composition of the sample. For all humid BSA containing samples two endothermic peaks can be observed, a *low*-temperature endothermic peak (T_d BSA 1), and a *high*-temperature endothermic peak (T_d BSA 2). It can be shown that the peak temperature of the low-temperature peak is inversely proportional to the moisture content (data not shown) and disappears entirely for absolutely dry BSA samples. The observed *high*-temperature endothermic

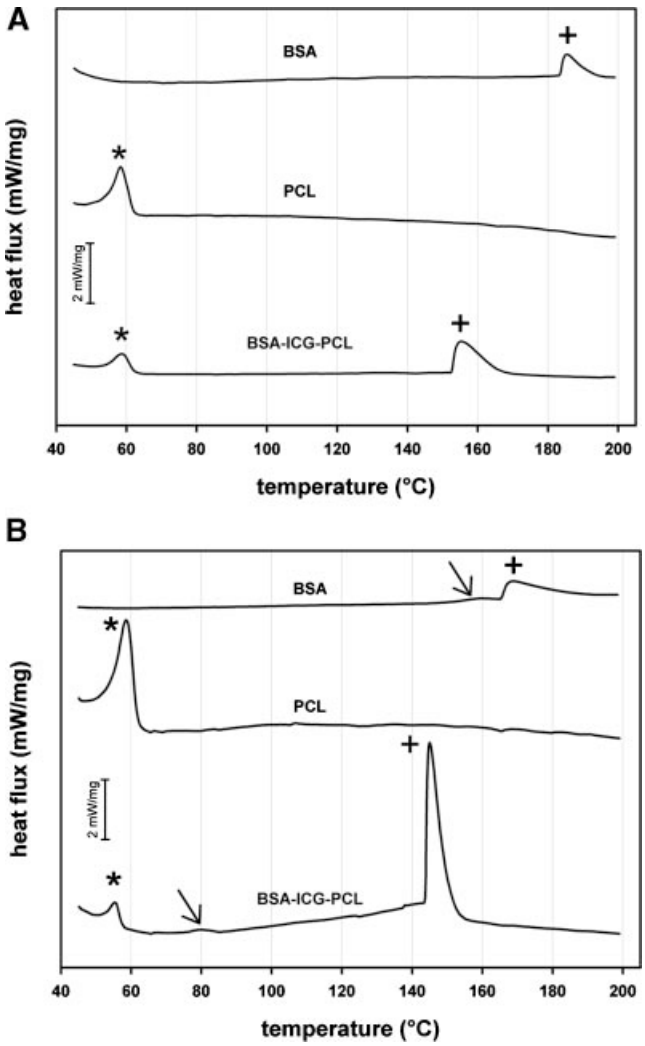

Fig. 6. DSC scans for BSA, PCL and BSA-ICG-PCL equilibrated at 25°C. (**A**) dried and (**B**) wet (5–15% water content) sample. The PCL melting point (T_m, marked by *) in any polymer containing composition is around 60°C. In wet BSA containing samples, two endothermic peaks are observed. Both endothermic peaks (lower (arrow), higher (+)) depend strongly on the water content [37] and presence of PCL/ICG.

peak (T_d BSA 2) depends strongly on the water content and the presence of PCL and/or ICG. Both peaks (T_d BSA 1 and 2) shift to lower temperatures with increasing water content and upon addition of PCL and/or ICG.

Histology

Light microscopy indicated thermal-related changes in the soldered vessels in an anatomically defined and reproducible pattern (Fig. 7). In treated aorta, unambiguous heat-induced cell death and coagulation of connective tissue matrix components were found to be restricted to the adventitia and its interface with the outermost layer of the tunica media. While partial dehydration during the procedure would occasionally result in slight compaction of medial layers, neither fragmentation of elastic lamina nor loss of nuclear staining were evident in such areas (Fig. 7C1,C2). The intimal layer is reflected as intact (Fig. 7C1,C2). At the interface between scaffold and tissue the melted PCL is found to create a smooth sealing (Fig. 7C3). Conversely, in overheated controls the entire thickness of the aortic wall resulted in shrinkage and/or vacuolation (Fig. 7D1,D2).

DISCUSSION

Aim of our study was to optimize adhesion properties regarding reproducibility and tensile strength in tissue soldering of rabbit aortic arteries and to further improve our intraluminal end-to-end soldering technique [33]. Controllable factors such as irradiation, preparation of tissue or production of polymer scaffolds have been standardized, allowing a precise measuring of influences such as BSA concentration or surface temperature.

Literature has shown that the use of a biodegradable polymer helps to improve tensile strength in tissue soldering [7,29,31]. In our study, PCL was the used polymer because of its low melting point at around 60°C [36]. We postulated to obtain a more homogenous and therefore stronger polymer–BSA–tissue-interaction by melting the polymer at the interface. The histologies (Fig. 7C1–C3) clearly show that the melted PCL creates a smooth sealing at the interface between scaffold and tissue, which we assume is an important factor to achieve good and reproducible tensile strengths. A further beneficial effect of the porous structure of our PCL-scaffold was that drying of the solder-soaked polymer prevented a runaway of the liquid solder during the heating process, which is an important prerequisite to clinical applications [35]. Production of the polymer was overall easy, however, when using the 40% BSA solder, the resulting scaffold was more difficult to process and more brittle as end product. The third beneficial effect of the polymer scaffold is that different thicknesses or shapes such as tubes can be realized to optimally adapt the scaffold to the surgical requirements.

Our measurements indicated that a higher energy deposition (either due to increasing power or irradiation time) resulted in stronger tissue bonds up to a maximum at which further irradiation did not lead to higher tensile strengths. This fact can be understood when analyzing the histologies. The stronger heating leads to an almost homogeneous intermixture of melted and denaturated BSA doped scaffold and thermally coagulated vessel wall tissue responsible for the increase in tensile strength, but at the expense of extensive tissue damage spread over the entire thickness of the vessel wall (Fig. 7D1,D2). The high temperature causes boiling of the tissue water resulting in a pronounced shrinkage and/or appearance of vacuoles in the tissue. As a result, the maximum tensile strength obtained levels off or even decreases as shown in Figure 3. The comparison of laser power and irradiation time in combination with macroscopic and histological evaluation revealed that using an irradiation power of 1.5 W and irradiation time of 60 seconds, a clinically practicable time, resulted in tensile strengths of about 2,000 mN. The associated tissue damage was restricted to the adventitia and its interface with the outermost layer of the tunica media without evidence of dehydration (Fig. 7). No damage of the intima was found. These settings were therefore regarded as optimal for further in vivo soldering experiments. The maximal polymer surface temperature was around 117°C. The ICG concentration was chosen to obtain the most homogenous absorption over the entire scaffold thickness [27]. Since ICG is the main absorber in the scaffold, no significant difference in end-temperature was measured using either the 25% or the 40% BSA scaffold.

The DSC-measurements (Fig. 6) revealed that the BIP-scaffold undergoes several thermodynamic changes upon heating. The lowest temperature peak (T_m PCL) was identified as the melting point of the PCL-scaffold. For all humid BSA containing samples two endothermic peaks can be observed, a *low*-temperature endothermic peak (T_d BSA 1), and a *high*-temperature endothermic peak (T_d BSA 2). The *low*-temperature peak (T_d BSA 1) appears over a wide range of temperatures (80–180°C) and corresponds to the denaturation of BSA [37]. This peak is highly dependent on the moisture content. The process leading to the *high*-temperature peak (T_d BSA 2), which appears over a temperature range from 140 to 185°C could not be fully explained. However, it has been shown that various types of DSC curves (single peak, single peak with shoulder, biomodal peaks, and two separate peaks) have been observed depending on the conditions [38]. For example, β-lactoglobulin shows an additional high-temperature peak near 140°C, which is related to the destabilization of the structure induced by a breakdown of disulfide bonds [39]. We suggest that the observed high temperature peak (T_d BSA 2) is an additional step in the denaturation process.

As previously shown, only temperatures in excess of 70°C lead to irreversible denaturation of BSA [39,40], but even then substantial amount of structures are retained. Therefore tissue soldering requires temperatures significantly higher than 70°C, since irreversible denaturation of BSA is assumed to be the main mechanism responsible for tissue connection.

The importance of the complete denaturation of the albumin to laser soldering is not well known. However, in order to provide long-term wound closure, it is very important

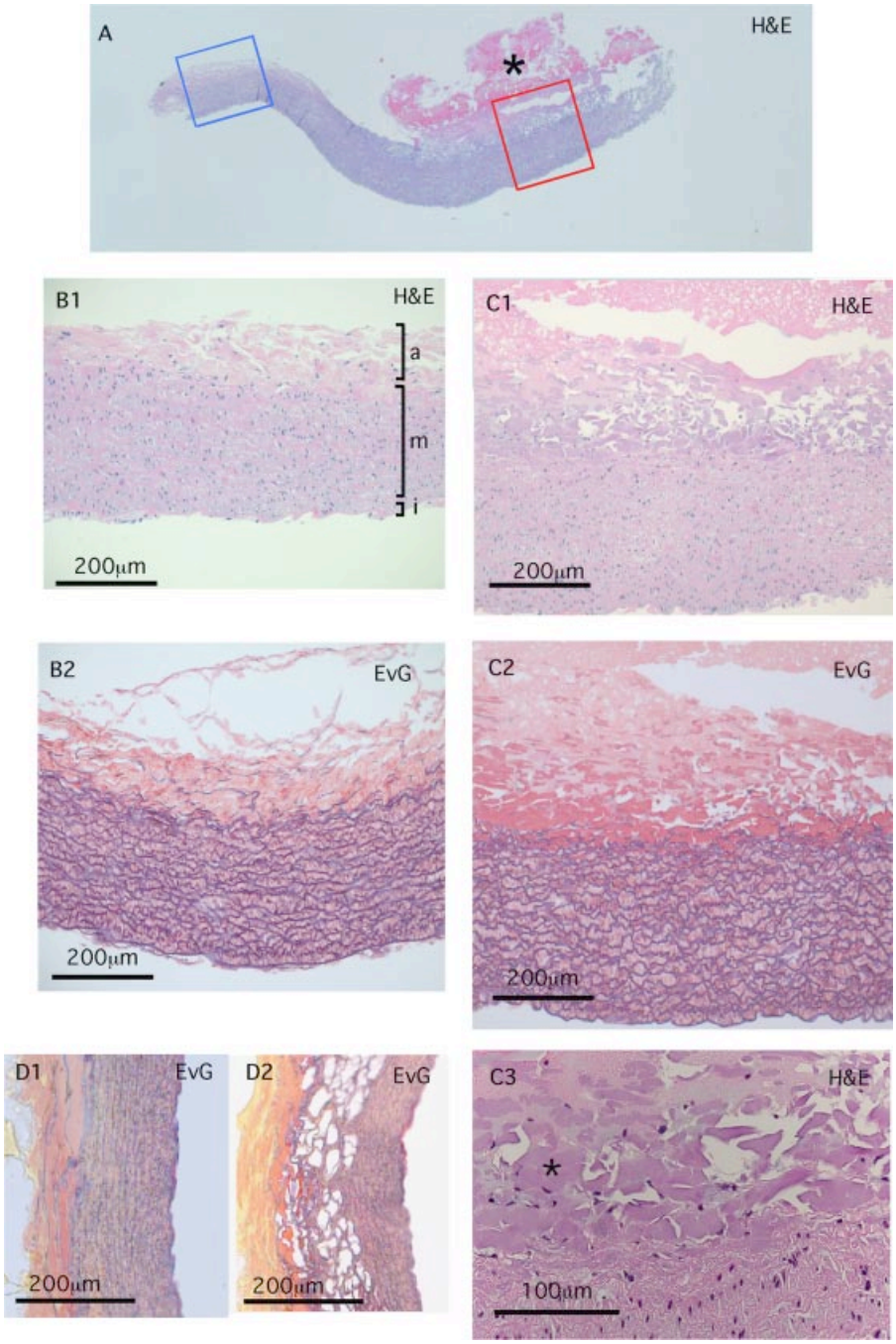

Fig. 7. Histology of vessel wall alterations locally induced by thermal effects of soldering at different soldering parameters (Fig. 3, asterisks). Histology is shown in H&E for assessment of cellular structural integrity. Van Gieson's elastic (EvG) is used for determination of the collagen matrix structure. **A**: Longitudinal whole-mount sections of rabbit aorta to show crust-like layer of coagulated soldering medium (asterisk) adherent to adventitia. Blue and red boxes indicate untreated control segment and soldered areas, respectively. **B1**,**B2**: Detail view of native aortic wall architecture corresponding to the blue box in A. The intima (i) being rather nondescript, the thickness of this large artery is mostly comprised of a robust tunica media (m) replete with undulating elastic fibers among which smooth muscle cells and fibroblasts are encased. Some of the elastic fibers along the outermost medial layer tend to gradually merge into the loose connective tissue of the adventitia (a). Note that interspersed nuclei of individual adventitial cells are clearly recognizable. **C1**,**C2**: Using optimum soldering parameters (1.5 W and 60 seconds) a thermal damage in the soldered area to adventitia is evident (red box in A). In comparison to B1, most adventitial nuclei have disappeared, and collagen as well as elastic fibers tends to form a poorly structured amalgam. Conversely, the tunica media (i.e., the most dynamically relevant layer) appears largely unaffected by coagulative changes. A full set of morphologically intact nuclei is appreciated in C1. The intima is appreciated as intact in C1,C2. In **C3** a higher magnification of C1, the melted BIP-scaffold (*) creates a smooth sealing of tissue and scaffold at their interface. Overheating (using soldering parameters of 1.5 W and 240 seconds), tended to produce shrinkage (**D1**) and/or vacuolation (**D2**).

that the solder is converted from a soluble to an insoluble form [41]. It is likely that this conversion occurs during the denaturation process, which is affected by many parameters. The effects of PCL and ICG on BSA denaturation have not been reported yet. However, it has been reported that pH variations, purity grade and additives can change shape and temperature range of BSA denaturation peak in DSC [39,42–44]. Antonov and Wolf [44] have shown in a BSA-polysaccharide system a shift of denaturation peak towards lower temperatures with increasing polymer concentration. An explanation is given that water structure is affected by the presence of the polymer, thus weakening the hydrophobic interactions in the tertiary structure of the protein. Moisture content affects protein denaturation accordingly and its effect has since long been observed and reported [45,46]. The used solder scaffolds are dry when placed on the wound; however the water content in the solder material increases with time due to adsorption and diffusion. We therefore assume that BSA undergoes a complete first denaturation reaction (T_d BSA 1) everywhere in the scaffold. It is also likely that the second observed denaturation reaction occurs near the scaffold-tissue interface, where moisture content is supposed to be highest. This results in a gradient of the denaturation temperature over the thickness of the polymer scaffold, which strongly supports the soldering process. Cellular integrity during the soldering procedure especially in the inner segments of the vessel is the primary goal, which can be achieved by keeping soldering temperature low. We have shown that by increasing the moisture the denaturation temperature can be reduced. Lowering pH slightly, adding a hydrophilic substance or using a protein mixture such as albumin and globulin may further reduced the effective soldering temperature [47].

Different previous studies have shown that increasing BSA concentration results in stronger tensile strengths [48,49]. Our experiments confirm this behavior. We found about 30% higher tensile strengths for the 40% BSA polymer scaffold compared to the 25% BSA scaffold. In absolute values the tensile strengths measured was around 2,000 mN when using the optimum settings and the 40% BIP-scaffold. As native, non-irradiated vessels have a tensile strength of approximately 3,800 mN, the dried solder doped BIP-scaffold showing rupture forces of more than 5,000 mN seems to be a perfect solid solder for further in vivo experiments since more than half of native strength can be achieved. Since all the ruptures happened at the interface between the vessel wall and the scaffold, we can expect that the tensile strength of a soldered end-to-end vascular anastomosis could even be enlarged when increasing the contact area. As we have developed a promising tissue adhesion matrix, the next step will be to show the feasibility of this soldering procedure in vivo and to evaluate long-term effects of the soldering regarding healing strength and patency.

Alternatives to Laser Tissue Soldering and Future Implications

The global surgical wound closure market is a large and fast growing medical field especially as treatment strategies tend toward more minimal invasive procedures such as endoscopy. Different materials are available. Fibrin based materials do not reach sufficient tensile strength and adhesion is of limited duration [50]. Synthetic substances such as acrylate based adhesives do obtain sufficient tensile strength but applicability is problematic as the physical properties change immediately on tissue contact in an irregular fashion. Another synthetic product such as polyethylene glycol has the property to swell up to 4 times its volume after application, and is thus unsuitable for a vascular clinical application. In all instructions for use of products available on the market, none releases the product as a substitute for sutures. The basic problems of tissue soldering are that the tissue fusion is either not strong enough, applicable only for large defects but imprecise for vascular anastomoses, or if strong enough then toxic. The medical request for a vascular anastomosis is that it can be performed in a reasonable time, meaning in the range of minutes. Mechanical devices have been promising and some functioning devices are already in clinical use. Unfortunately, they are limited to relative large vessels preventing minimally invasive applications [36,51]. Promising on the other hand are adhesion matrices, which can either be activated by laser irradiation or by an electromagnetic field [52]. PCL as matrix basis seems to be an auspicious material since its biocompatibility has already been shown (FDA approved), 3D modeling is possible and handling is simple.

CONCLUSION

Rabbit aortic arteries have been successfully soldered using an 808 nm diode laser and an ICG-BSA-PCL-scaffold (BIP-scaffold). The polymer scaffold was soaked either with a 25% or 40% BSA solder and then air-dried. Different irradiation parameters were tested and analyzed for tensile strength and histological tissue damage. Optimal irradiation settings were assigned based on strong and reproducible tensile strengths with minimal thermal damage. The irradiation time was chosen to be feasible for medical purposes. The 40% BSA polymer scaffold resulted in a tensile strength of about 2,000 mN, which is more than half of the native non-irradiated vessel rupture force. The soldered vessels showed circumscribed damage of adventitia without evidence of dehydration and preservation of the cellular structure of the medial layer of the aorta. The combination of BSA, PCL, and ICG positively influences the soldering process by significantly lowering the denaturation temperature of BSA. The BIP-scaffold enables a defined solder deposition and fixation of absorber to the region of interest resulting in reproducible and strong tensile strengths.

ACKNOWLEDGMENTS

We thank Rosmarie and Felix Näf, KaniSwiss GmbH, Thörigen, Switzerland, for providing us the rabbit aortas. Further we thank Eva Krähenbühl, René Nyffenegger and Andreas Friedrich, Institute of Applied Physics, Bern, Switzerland and Prof. Hans-Rudolf Widmer,

Neurosurgery, Bern, Switzerland for their support. Michael Reinert and Amadé Bregy are supported by the Swiss National Foundation (Grant No. 3200B0-107611).

REFERENCES

1. Zeebregts C, van den Dungen J, Buikema H, van der Want J, van Schilfgaarde R. Preservation of endothelial integrity and function in experimental vascular anastomosis with non-penetrating clips. Br J Surg 2001;88(9):1201–1208.
2. Macchiarelli G, Familiari G, Caggiati A, Magliocca FM, Riccardelli F, Miani A, Motta PM. Arterial repair after microvascular anastomosis. Scanning and transmission electron microscopy study. Acta Anat (Basel) 1991;140(1): 8–16.
3. Pagnanelli DM, Pait TG, Rizzoli HV, Kobrine AI. Scanning electron micrographic study of vascular lesions caused by microvascular needles and suture. J Neurosurg 1980;53(1): 32–36.
4. Zeebregts CJ, Heijmen RH, van den Dungen JJ, van Schilfgaarde R. Non-suture methods of vascular anastomosis. Br J Surg 2003;90(3):261–271.
5. Lidman D, Daniel RK. The normal healing process of microvascular anastomoses. Scand J Plast Reconstr Surg 1981;15(2):103–110.
6. Zeebregts CJ, van den Dungen JJ, Kalicharan D, Cromheecke M, van der Want J, van Schilfgaarde R. Nonpenetrating vascular clips for small-caliber anastomosis. Microsurgery 2000;20(3):131–138.
7. Sorg BS, Welch AJ. Preliminary biocompatibility experiment of polymer films for laser-assisted tissue welding. Lasers Surg Med 2003;32(3):215–223.
8. Bass LS, Treat MR. Laser tissue welding: A comprehensive review of current and future clinical applications. Lasers Surg Med 1995;17(4):315–349.
9. Walz JM, Paterson CA, Seligowski JM, Heard SO. Surgical site infection following bowel surgery: A retrospective analysis of 1446 patients. Arch Surg 2006;141(10):1014–1018.
10. Basu S, Marini CP, Bauman FG, Shirazian D, Damiani P, Robertazzi R, Jacobowitz IJ, Acinapura A, Cunningham JN Jr. Comparative study of biological glues: Cryoprecipitate glue, two-component fibrin sealant, and "French" glue. Ann Thorac Surg 1995;60(5):1255–1262.
11. Park W, Kim WH, Lee CH, Kim DY, Choi JH, Huh JW, Sung HM, Kim IS, Kweon OK. Comparison of two fibrin glues in anastomoses and skin closure. J Vet Med A Physiol Pathol Clin Med 2002;49(7):385–389.
12. Green AR, Milling MA, Green AR. Butylcyanoacrylate adhesives in microvascular surgery: An experimental pilot study. J Reconstr Microsurg 1986;2(2):103–105.
13. Mitsuhata H, Horiguchi Y, Saitoh J, Saitoh K, Fukuda H, Hirabayasi Y, Togashi H, Shimizu R. An anaphylactic reaction to topical fibrin glue. Anesthesiology 1994;81(4): 1074–1077.
14. Berguer R, Staerkel RL, Moore EE, Moore FA, Galloway WB, Mockus MB. Warning: Fatal reaction to the use of fibrin glue in deep hepatic wounds. Case reports. J Trauma 1991; 31(3):408–411.
15. McNally K, Welch A. Laser tissue welding. In: Vo-Dinh T, editor. Biomed photonics. London: CRC 2003. Ch. 39, 1–45.
16. Yahr WZ, Strully KJ, Hurwitt ES. Non-occlusive small arterial anastomosis with a neodymium laser. Surg Forum 1964;15:224–226.
17. Jain KK, Gorisch W. Repair of small blood vessels with the neodymium-YAG laser: A preliminary report. Surgery 1979; 85(6):684–688.
18. Baggish MS, Chong AP. Carbon dioxide laser microsurgery of the uterine tube. Obstet Gynecol 1981;58(1):111–116.
19. White RA, White GH, Fujitani RM, Vlasak JW, Donayre CE, Kopchok GE, Peng SK. Initial human evaluation of argon laser-assisted vascular anastomoses. J Vasc Surg 1989;9(4): 542–547.
20. McKennan KX. "Tissue welding" with the argon laser in middle ear surgery. Laryngoscope 1990;100(11):1143–1145.
21. Rebeiz E. Preliminary clinical results of window partial laryngectomy: A combined endoscopic and open technique. Ann Otol Rhinol Laryngol 2000;109(12 Pt 1):1176.
22. Dogra PN, Nabi G. Laser welding of vesicovaginal fistula. Int Urogynecol J Pelvic Floor Dysfunct 2001;12(1):69–70.
23. Kirsch AJ, Cooper CS, Gatti J, Scherz HC, Canning DA, Zderic SA, Snyder HM III. Laser tissue soldering for hypospadias repair: Results of a controlled prospective clinical trial. J Urol 2001;165(2):574–577.
24. Kirsch AJ, de Vries GM, Chang DT, Olsson CA, Connor JP, Hensle TW. Hypospadias repair by laser tissue soldering: Intraoperative results and follow-up in 30 children. Urology 1996;48(4):616–623.
25. Kirsch AJ, Miller MI, Hensle TW, Chang DT, Shabsigh R, Olsson CA, Connor JP. Laser tissue soldering in urinary tract reconstruction: First human experience. Urology 1995;46(2): 261–266.
26. Byrd BD, Heintzelman DL, McNally-Heintzelman KM. Absorption properties of alternative chromophores for use in laser tissue soldering applications. Biomed Sci Instrum 2003;39:6–11.
27. Ott B, Zuger BJ, Erni D, Banic A, Schaffner T, Weber HP, Frenz M. Comparative in vitro study of tissue welding using a 808 nm diode laser and a Ho:YAG laser. Lasers Med Sci 2001;16(4):260–266.
28. McNally KM, Sorg BS, Chan EK, Welch AJ, Dawes JM, Owen ER. Optimal parameters for laser tissue soldering: II. Premixed versus separate dye-solder techniques. Lasers Surg Med 2000;26(4):346–356.
29. Hoffman GT, Soller EC, McNally-Heintzelman KM. Biodegradable synthetic polymer scaffolds for reinforcement of albumin protein solders used for laser-assisted tissue repair. Biomed Sci Instrum 2002;38:53–58.
30. Sorg BS, Welch AJ. Tissue welding with biodegradable polymer films-demonstration of acute strength reinforcement in vivo. Lasers Surg Med 2002;31(5):339–342.
31. Sorg BS, Welch AJ. Laser-tissue soldering with biodegradable polymer films in vitro: Film surface morphology and hydration effects. Lasers Surg Med 2001;28(4):297–306.
32. Lauto A, Foster LJ, Ferris L, Avolio A, Zwaneveld N, Poole-Warren LA. Albumin-genipin solder for laser tissue repair. Lasers Surg Med 2004;35(2):140–145.
33. Ott B, Constantinescu MA, Erni D, Banic A, Schaffner T, Frenz M. Intraluminal laser light source and external solder: In vivo evaluation of a new technique for microvascular anastomosis. Lasers Surg Med 2004;35(4):312–316.
34. Wake MC, Gupta PK, Mikos AG. Fabrication of pliable biodegradable polymer foams to engineer soft tissues. Cell Transplant 1996;5(4):465–473.
35. McNally KM, Sorg BS, Welch AJ. Novel solid protein solder designs for laser-assisted tissue repair. Lasers Surg Med 2000;27(2):147–157.
36. Yang S, Leong KF, Du Z, Chua CK. The design of scaffolds for use in tissue engineering. Part I. Traditional factors. Tissue Eng 2001;7(6):679–689.
37. Farahnaky A, Badii F, Farhat IA, Mitchell JR, Hill SE. Enthalpy relaxation of bovine serum albumin and implications for its storage in the glassy state. Biopolymers 2005;78(2):69–77.
38. deWit JN, Klarenbeek G. Effects of various heat treatments on structure and solubility of whey proteins. J Dairy Sci 1984;67(11):2701–2710.
39. Michnik A. Thermal stability of bovine serum albumin DSC study. J Therm Anal Calorim 2003;71:509–519.
40. Clark A, Richardson R, Robinson G, Ross-Murphy S, Weaver A. Structure and mechanical properties of agar/BSA co-gels. Progr Food Nutri Sci 1982;6:11.
41. Bleustein CB, Sennett M, Kung RT, Felsen D, Poppas DP, Stewart RB. Differential scanning calorimetry of albumin solders: Interspecies differences and fatty acid binding effects on protein denaturation. Lasers Surg Med 2000;27(5):465–470.
42. Yamasaki M, Yano H, Aoki K. Differential scanning calorimetric studies on bovine serum albumin: I. Effects of

pH and ionic strength. Int J Biol Macromol 1990;12(4):263–268.
43. Michnik A, Michalik K, Drzazga Z. Stability of bovine serum albumin at different pH. J Therm Anal Calorim 2005;80:399–406.
44. Antonov YA, Wolf BA. Calorimetric and structural investigation of the interaction between bovine serum albumin and high molecular weight dextran in water. Biomacromolecules 2005;6(6):2980–2989.
45. Tsukada H, Takano K, Hattori M, Yoshida T, Kanuma S, Takahashi K. Effect of sorbed water on the thermal stability of soybean protein. Biosci Biotechnol Biochem 2006;70(9): 2096–2103.
46. Barker H. The effect of water content upon the rate of heat denaturation of crystallizable egg albumin. J Gen Physiol 1933;17(1):21–34.
47. Sanchez del Angel S, Moreno Martinez E, Valdivia Lopez M. Study of denaturation of corn proteins during storage using differential scanning calorimetry. Food Chem 2003; 83(4):9.
48. McNally KM, Sorg BS, Chan EK, Welch AJ, Dawes JM, Owen ER. Optimal parameters for laser tissue soldering. Part I: Tensile strength and scanning electron microscopy analysis. Lasers Surg Med 1999;24(5):319–331.
49. Lauto A. Repair strength dependence on solder protein concentration: A study in laser tissue-welding. Lasers Surg Med 1998;22(2):120–125.
50. Knecht S, Erggelet C, Endres M, Sittinger M, Kaps C, Stussi E. Mechanical testing of fixation techniques for scaffold-based tissue-engineered grafts. J Biomed Mater Res 2007; 83(1):50–57.
51. Bregy A, Alfieri A, Demertzis S, Mordasini P, Jetzer AK, Kuhlen D, Schaffner T, Dacey R, Steiger HJ, Reinert M. Automated end-to-side anastomosis to the middle cerebral artery: A feasibility study. J Neurosurg 2008;108(3):567–574.
52. Bregy A, Kohler A, Steitz B, Petri-Fink A, Bogni S, Alfieri A, Münker M, Vajtai I, Frenz M, Hofmann H, Reinert M. Electromagentic tissue fusion using superparamagnetic iron oxide nanoparticles: First experience with rabbit aorta. Open Surg J 2008;2:6.